

On Fading Channel Dependency Structures with a Positive Zero-Outage Capacity

Karl-Ludwig Besser, *Student Member, IEEE*, Pin-Hsun Lin, *Member, IEEE*, and Eduard A. Jorswieck, *Fellow, IEEE*

Abstract—With emerging wireless technologies like 6G, many new applications like autonomous systems evolve which have strict demands on the reliability and latency of data communications. In the scenario of the commonly investigated independent slow fading links, the zero-outage capacity (ZOC) is zero and retransmissions are therefore inevitable. In this work, we show that a positive ZOC can be achieved under the same setting of slow fading with constant transmit power and without perfect channel state information at the transmitter, if the joint distribution of the channel gains follows certain structures. This allows reliable reception without any outages, thus not requiring retransmissions. Based on a systematic copula approach, we show that there exists a set of dependency structures for which positive ZOCs can be achieved for both maximum ratio combining (MRC) and selection combining (SC). We characterize the maximum ZOC within a finite number of bits. The results are evaluated explicitly for the special cases of Rayleigh fading and Nakagami- m fading in order to quantify the ZOCs for common fading models.

Index Terms—Copula, Joint distributions, Fading channels, Delay-limited capacity, Outage probability.

I. INTRODUCTION

Current visions for emerging technologies like 6G include new applications like autonomous systems which have extremely high reliability constraints [2], [3]. It is therefore of great interest, how these strict reliability constraints can be achieved.

For slow-fading channels, a common performance metric is the ε -outage capacity. It is defined as the maximum transmission rate for which the outage probability is not greater than ε . Of particular interest is the zero-outage capacity (ZOC), i.e., the maximum transmission rate at which we can transmit *without any* outages. This will be especially relevant in the context of ultra-reliable low latency communication (URLLC) [3]–[5].

It is well-known that the ZOC is zero in most of the common scenarios considered in the literature, e.g., single link single-input single-output (SISO) with independent Rayleigh fading [6]. In [7], it is shown that a negative correlation improves the outage probability compared to independent channels. The authors consider the special scenario of a dual-branch system with linearly correlated log-normal fading channels. A similar observation is made

in [8]. Furthermore, it was shown in [9], that the ZOC can be positive for two Rayleigh fading links without perfect channel-state information at the transmitter (CSI-T), if the two channels are negatively correlated. Taking more general dependency structures into account, bounds on the ε -outage capacity for communication systems with n dependent fading links are derived in [10]. It is shown that the upper-bound on the ε -outage capacity, i.e., for the best-case joint distribution, is strictly positive. This implies that there exists at least one joint distribution for which the ZOC is positive for given arbitrary marginals. However, it remains an open question, if there exist multiple joint distributions that achieve a positive ZOC. Additionally, it is unclear, if there exist joint distributions for which the ZOC is positive but strictly less than the upper bound derived in [10]. A positive ZOC implies that a transmission without any outages is possible. This is relevant, e.g., in the context of URLLC, since no retransmissions are necessary which allows a very low latency. Besides, if there exists only a single joint distribution with a positive ZOC, this would be an unstable operating point. We are therefore also interested in other joint distributions achieving positive ZOCs.

In this work, we will answer both of these open questions: We show that there exists an infinite number of joint distributions, for which the ZOC is strictly between zero and the best-case upper bound. The proof is constructive in the way that we explicitly give a parametrized family of joint distributions that achieve positive ZOCs. Our results hold for general fading distributions, and are evaluated for the special case of Rayleigh fading and Nakagami- m fading.

From the results of this work and previous work, e.g., [10], it becomes apparent that the outage performance of communication systems can be significantly improved by dependent channels. In view of the strict reliability requirements that current and future 6G applications have [5], [11], this indicates that active dependency control is a promising direction of research to enable ultra-reliable communications. Emerging technologies like reconfigurable intelligent surfaces (RISs) [12] could allow for such an active dependency control.

This work is concerned with the theoretical limits of the outage performance for dependent fading channels, which will serve as an upper bound for practical and heuristic future communication system designs. The basis of our derivations is copula theory [13], which allows a flexible modeling of dependency structures between random variables. Copulas have been used in communications before to model dependency between channels. One of the first works on applying this technique in the context of wireless communications is [14]. There, a Clayton copula is used to introduce a new

Parts of this work have been presented at the 54th Asilomar Conference on Signals, Systems, and Computers, November 2020 [1].

The authors are with the Institute of Communications Technology, Technische Universität Braunschweig, 38106 Braunschweig, Germany (email: {k.besser, p.lin, e.jorswieck}@tu-bs.de).

The work of K.-L. Besser is supported in part by the German Research Foundation (DFG) under grant JO 801/23-1. The work of E. Jorswieck is supported in part by DFG under grant JO 801/25-1.

fading model for Nakagami- m fading with tail dependence. In [15], [16], copulas have been used to model dependency in multiple-input multiple-output (MIMO) channels. In [17], it was shown on measurements that real channels can show a tail dependency which can be described by copulas. The outage probability of the two-user Rayleigh fading multiple access channel (MAC), where the two links follow a specific copula, is evaluated in [18]. Copulas have also been used to model interference in internet of things (IoT) networks [19] and in the area of physical layer security [20]–[22]. General bounds on the outage performance for dependent slow-fading channels can be found in [23].

The tools from copula theory are not only helpful for analyzing the outage capacity for slow fading channels, but also for the ergodic capacities for fast fading multi-user channels [24]. In particular, when the multi-user channel has the same marginal property, copulas have been used to derive capacities regions for Gaussian interference channels, Gaussian broadcast channels and the secrecy capacity for Gaussian wiretap channels [25]–[27].

However, in this work, we focus on the ZOC for n dependent slow-fading links. Our contributions are summarized as follows.

- We show that the ZOC in a multi-connectivity setting can be strictly positive for dependent channels with arbitrary marginal fading distributions, even when only statistical CSI-T is available and a constant transmit power is used. We consider both maximum ratio combining (MRC) and selection combining (SC) at the receiver.
- We show that the ZOC is maximized by countermonotonic channel gains in the case of two dimensions. For the general case, we show that there exists an infinite number of joint distributions, for which the ZOC is strictly between zero and the best-case (upper) bound. The proof is constructive in the way that we explicitly state a parameterized family of joint distributions that achieve positive ZOCs.
- We provide an explicit expression for the maximum ZOC for SC at the receiver with n homogeneous links. For n heterogeneous links, we give an implicit characterization of the maximum ZOC.
- We derive inner and outer bounds for the maximum ZOC in the general case of $n > 2$ channels with homogeneous channel gains X and MRC at the receiver. The bounds are within a finite gap for all n equal to $\log_2(\mathbb{E}[X]) - \log_2(F_X^{-1}(1/e))$.
- All results are evaluated for the special cases of Rayleigh fading and Nakagami- m fading. In addition, we provide all plots presented in this work as interactive versions in [28].

The practical implications of the results are the following. If one is able to tune the dependency structure between different channels, e.g., by using smart relays [29] or reconfigurable meta-surfaces [12], it is possible to transmit data over fading channels without any outages. The second result implies a certain robustness. Assume that we are able to parameterize the dependency structure within a desired range. Even if

the designed parameters are not set perfectly, the ZOC can still be positive, if one hits one of the infinitely many joint distributions with positive ZOC.

The rest of the paper is organized as follows. In Section II, we state the system model and problem formulation of this work. We also introduce some necessary mathematical background from copula theory. Some general observation and results are given in Section III. The two diversity combining techniques MRC and SC are investigated in detail in Sections IV and V, respectively. Finally, Section VI concludes the paper.

Notation: Throughout this work, we use the following notation. Random variables are denoted in capital letters, e.g., X , and their realizations in small letters, e.g., x . Vectors are written in boldface letters, e.g., \mathbf{X} . We use F and f for a probability distribution and its density, respectively. The expectation is denoted by \mathbb{E} and the probability of an event by \Pr . It is assumed that all considered distributions are continuous. The uniform distribution on the interval $[a, b]$ is denoted as $\mathcal{U}[a, b]$. The normal distribution with mean μ and variance σ^2 is denoted as $\mathcal{N}(\mu, \sigma^2)$. The derivative of a function f is denoted by f' . As a shorthand, we use $[x]^+ = \max[x, 0]$. The real numbers, non-negative real numbers, and extended real numbers are denoted by \mathbb{R} , \mathbb{R}_+ , and $\bar{\mathbb{R}}$, respectively. Logarithms, if not stated otherwise, are assumed to be with respect to the natural base.

II. PRELIMINARIES AND SYSTEM MODEL

We consider a slow fading channel with n receive antennas. The symbol $M \in \mathbb{C}$ is transmitted with a rate R over the slow fading links $H_i \in \mathbb{C}$, $i = 1, \dots, n$. The received signal $\mathbf{Y} = (Y_1, \dots, Y_n) \in \mathbb{C}^n$ is given as

$$Y_i = H_i M + N_i, \quad (1)$$

where N_i are independent complex Gaussian noise terms with zero mean and variance σ_i^2 . The transmit signal-to-noise ratios (SNRs) of the individual channels are given as $\rho_i = P/\sigma_i^2$, where P is the average transmit power constraint.

We assume that the receiver has perfect channel-state information (CSI) while the transmitter only has statistical CSI. The receiver applies the diversity combining strategy $L: \mathbb{R}_+^n \rightarrow \mathbb{R}$. In this work, we consider strategies in the form $L(X_1, \dots, X_n)$ with $X_i = \rho_i |H_i|^2$. In this case, an outage occurs, if the instantaneous channel capacity is less than the rate R used for the transmission, i.e., $\log_2(1 + L(X_1, \dots, X_n)) < R$. The maximum rate R^ε for which the probability of such an outage is less than ε is called ε -outage capacity and defined as [6]

$$R^\varepsilon = \sup_{R \geq 0} \left\{ R \mid \Pr \left(\log_2(1 + L(X_1, \dots, X_n)) < R \right) \leq \varepsilon \right\}. \quad (2)$$

This can be reformulated as the (receive) SNR optimization

$$s^*(\varepsilon) = \sup_{s \geq 0} \{s \mid \Pr(L(X_1, \dots, X_n) < s) \leq \varepsilon\} \quad (3)$$

with $R^\varepsilon = \log_2(1 + s^*(\varepsilon))$.

A. Problem Formulation

We consider a communication scenario with n slow-fading channels which can be dependent. The receiver has perfect CSI, while we only assume statistical CSI-T. The quantity of interest is the zero-outage capacity R^0 , which is given as the maximum rate fulfilling

$$\Pr\left(L(X_1, \dots, X_n) < 2^{R^0} - 1\right) = 0. \quad (4)$$

The main question that we will answer in this work is: *Given marginal distributions of the individual wireless fading channels, do there exist joint distributions (and how many) which achieve positive ZOCs and what ZOCs can be achieved by different diversity combining techniques?* As a consequence, this also includes the maximum ZOC with respect to all joint distributions with the given marginals.

By the construction in [10], we know that there exists at least one joint distribution with positive zero-outage capacity. However, a singleton is an unstable operating point and it is therefore of interest, how robust a positive ZOC is with respect to the joint distribution. In addition, we are interested in the maximum ZOC since it shows what the best case performance can be.

B. Mathematical Background

To describe and analyze the structure of joint distributions, we will use tools from copula theory [13], which we introduce in the following.

Definition 1 (Copula). A copula is an n -dimensional distribution function with standard uniform marginals.

The practical relevance of copulas stems from Sklar's theorem, which we restate in the following Theorem 1.

Theorem 1 (Sklar's Theorem [13, Thm. 2.10.9]). *Let H be an n -dimensional distribution function with margins F_1, \dots, F_n . Then there exists a copula C such that for all $x \in \bar{\mathbb{R}}^n$,*

$$H(x_1, \dots, x_n) = C(F_1(x_1), \dots, F_n(x_n)). \quad (5)$$

If F_1, \dots, F_n are all continuous, then C is unique. Conversely, if C is a copula and F_1, \dots, F_n are distribution functions, then H defined by (5) is an n -dimensional distribution function with margins F_1, \dots, F_n .

This theorem implies that copulas can be used to describe dependency structures between random variables, regardless of their marginal distributions. This allows us to separate the dependency structure (described by the copula C) from the marginal distributions F_1, \dots, F_n . We will see in the following section that the ZOC depends on the underlying copula between the channel gains. Some results in this work are based on the Fréchet-Hoeffding bounds for copulas, which we state in the following theorem.

Theorem 2 (Fréchet-Hoeffding Bounds [13, Thm. 2.10.12]). *Let C be a copula. Then for every $u \in [0, 1]^n$*

$$W(u) \leq C(u) \leq M(u) \quad (6)$$

with

$$W(u) = \max\{u_1 + \dots + u_n - n + 1, 0\}, \quad (7)$$

$$M(u) = \min\{u_1, \dots, u_n\}. \quad (8)$$

In the case that $n = 2$, W is a copula and two random variables whose joint distribution follows the copula W are called countermonotonic. The upper bound M is a copula for all n and random variables that follow M are called comonotonic [13].

III. GENERAL CONSIDERATIONS AND RESULTS

In this section, we will make some general observations and derivations about the considered problem. Throughout this work, we will assume that the diversity combining function L only depends on the channel gains $X_i = \rho_i |H_i|^2$ and is non-decreasing in each variable.

The underlying observation for our derivations in this work is the following. As stated in Section II, we know that the outage probability corresponds to the probability of the event $L(X_1, \dots, X_n) < s$. An equivalent way of expressing this is via the integral of the joint distribution F_{X_1, \dots, X_n} over the area

$$\mathcal{S} = \{(x_1, \dots, x_n) \in \mathbb{R}_+^n \mid L(x_1, \dots, x_n) < s\}. \quad (9)$$

Then the outage probability, given R , can be written as

$$\varepsilon = \int_{\mathcal{S}} dC(F_{X_1}(x_1), \dots, F_{X_n}(x_n)), \quad (10)$$

where we use the copula representation of the joint distribution based on Theorem 1.

Recall that our goal is to have zero outages, i.e., $\varepsilon = 0$. With reference to (10), this is achieved if the probability of the joint distribution is zero in \mathcal{S} . The joint cumulative distribution function (CDF) is zero if and only if its copula C is zero, and the corresponding area of (X_1, \dots, X_n) can be written as

$$\mathcal{B} = \{(x_1, \dots, x_n) \mid C(F_{X_1}(x_1), \dots, F_{X_n}(x_n)) = 0\}. \quad (11)$$

In other words, \mathcal{S} is not inside the support of (X_1, \dots, X_n) . This idea is exemplarily shown in Fig. 1 for the two diversity schemes MRC and SC. Detailed explanations and results for both diversity schemes will be given in the following sections.

A. Two-Dimensional Case

First, we show that the ZOC R^0 is upper bounded by countermonotonic channels for $n = 2$.

Corollary 3 (Maximum ZOC). *The maximum ZOC for two links with channel gains X_1 and X_2 is attained by countermonotonic random variables, i.e., their joint distribution follows copula W .*

Proof. The proof can be found in Appendix A. \square

Remark 1 (Minimum ZOC). It is well-known that the ZOC can be zero, e.g., for channels with independent links [6]. Since the capacity is a non-negative quantity, we can conclude that zero is the lower bound on the ZOC.

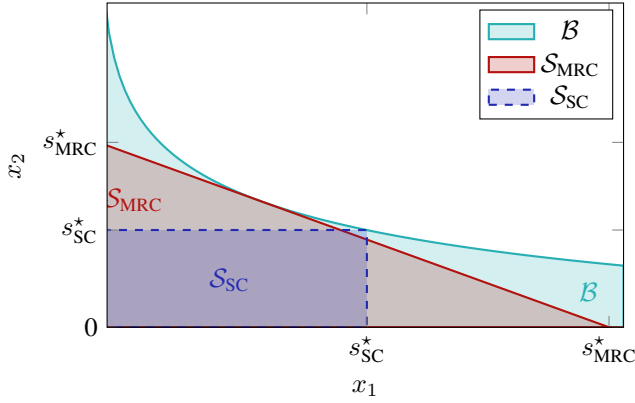


Figure 1. Areas corresponding to the ZOC. Area \mathcal{B} shows the area where $F_{X_1, X_2} = 0$. Area \mathcal{S}_{MRC} shows the integration area from (10) to calculate the outage probability when MRC is used at the receiver. The value s_{MRC}^* denotes the maximum value of s such that \mathcal{S}_{MRC} is still a subset of \mathcal{B} . The analogue for SC at the receiver is denoted by the index “SC”.

B. General Case

The extension to the general n -dimensional case with $n > 2$ is not straightforward, since W is only a valid copula for $n = 2$. However, we can reformulate the problem in the general case using the discussions from above. Our goal is to find the maximum value of R in (2) (or equivalently, s^* in (3)), such that \mathcal{S} is still a subset of \mathcal{B} . Note that the boundary of \mathcal{B} is not necessarily convex. We, therefore, rewrite the optimization problem (3) as

$$s^* = \max_{(x_1, \dots, x_n) \in \mathcal{B}} L(x_1, \dots, x_n).$$

Since we know from the monotonicity of L that the maximum will be on the boundary of \mathcal{B} defined by B , s^* can also be written as minimizing the function L over the boundary B as

$$s^* = \min_{(x_1, \dots, x_n)} L(x_1, \dots, x_n) \quad (12)$$

s.t. $B(x_1, \dots, x_n) = 0$.

The structure of the boundary function B is determined by the underlying joint distribution and we will give particular examples in the following sections. Throughout the rest of this work, we will assume that B is a smooth function.

IV. MAXIMUM RATIO COMBINING

First, we will investigate the case that the receiver applies MRC as the diversity combining technique. In this case, the combination function L is the sum of the channel gains X_i [6]

$$L_{\text{MRC}}(X_1, \dots, X_n) = \sum_{i=1}^n X_i.$$

In order to introduce the basic concepts, we will start with the two-dimensional case and then extend the results to the general n -dimensional case. The results will be illustrated with two examples, namely Rayleigh fading and Nakagami- m fading.

A. Two-Dimensional Case

We start with the two-dimensional case $n = 2$. From Corollary 3, we know that the maximum ZOC is attained for countermonotonic (X_1, X_2) . In the following theorem, we show that for each value c between zero and the maximum ZOC, there exists a joint distribution for which the ZOC is equal to c , i.e., the ZOC is continuous with respect to the joint distribution.

Theorem 4 (Zero-Outage Capacities for Two Links with MRC). *Let X_1 and X_2 be non-negative continuous random variables representing the channel gains of two communication links. The receiver applies MRC as the diversity combining technique. Then there exist joint distributions of X_1 and X_2 with the following zero-outage capacities for $t \in [0, 1]$*

$$R^0(t) = \log_2 \left(1 + \min \left\{ F_{X_1}^{-1}(t), F_{X_2}^{-1}(t), x^* + B_t(x^*) \right\} \right) \quad (13)$$

with

$$B_t(x) = F_{X_2}^{-1}(t - F_{X_1}(x)) \quad (14)$$

and

$$x^* = \arg \min_{x \geq 0} \left\{ x + B_t(x) \mid f_{X_1}(x) = f_{X_2}(F_{X_2}^{-1}(t - F_{X_1}(x))) \right\}. \quad (15)$$

Proof. The proof can be found in Appendix B. \square

The parameter t characterizes the joint distribution of the two fading links. For $t = 0$ and $t = 1$, X_1 and X_2 are comonotonic and countermonotonic, respectively. The maximum ZOC is therefore achieved for $t = 1$.

Remark 2 (Ambiguity of the Dependency Structure). In the proof of Theorem 4, we used the copula C_t from [13, Chap. 3.2.2]. However, the only property we actually require for the proof is the fact that $C_t(a, b) = 0$ for $a + b \leq t$. Thus, any copula, that has this property, achieves the same result. Another example having this property is a generalization of the circular copula [13, Eq. (3.1.5)]

$$C_{t, \text{circ}}(a, b) = \begin{cases} M(a, b) & \text{if } |a - b| > t \\ W(a, b) & \text{if } |a + b - 1| < 1 - t \\ \frac{a+b}{2} - \frac{t}{2} & \text{otherwise,} \end{cases}$$

which is illustrated in Fig. 9b in Appendix B. There are also families of absolutely continuous copulas whose support is not the full unit square. An example is the Clayton copula given by [13, Eq. (4.2.1)]

$$C_{\theta, \text{clay}}(a, b) = \left(\max [a^{-\theta} + b^{-\theta} - 1, 0] \right)^{-\frac{1}{\theta}},$$

with $\theta \in [-1, \infty) \setminus \{0\}$ for negative values of the parameter θ .

In Fig. 2, a numerical example to illustrate the structure of the joint distribution is shown where we show 2000 random samples of two Rayleigh fading channel gains with SNRs $\rho_1 = \rho_2 = 0$ dB. Their joint distribution in Fig. 2b follows the Clayton copula with $\theta = -0.75$. It can easily be seen that there are no realizations for which both channel gains are close to zero simultaneously. This enables a positive ZOC, cf. Fig. 1. In contrast, the ZOC is zero for independent channels as can be seen in Fig. 2a.

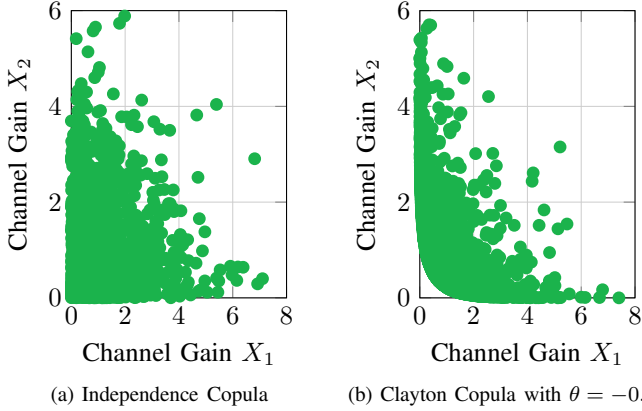


Figure 2. Random joint Rayleigh fading realizations with different copulas underlying the joint distribution. The SNR of both channel gains is set to $\rho = 0$ dB.

B. General Case

From Theorem 4, it can be seen that there exists an infinite number of joint fading distributions that achieve a positive ZOC. This answers the first part of our question from Section II-A and shows that the set of joint distributions with a positive ZOC is not a singleton. In the following, we will therefore only focus on the *maximum* ZOC with respect to the set of joint distributions.

As shown in Corollary 3, for the two-dimensional case, the maximum is achieved for countermonotonic channel gains, i.e., X_1 and X_2 follow the W -copula, cf. Theorem 2. Unfortunately, the extension to the general n -dimensional case is not straightforward since the Fréchet-Hoeffding lower bound W is not a copula anymore for $n > 2$. The most general case of arbitrary marginal distributions F_{X_1}, \dots, F_{X_n} with $n > 2$, therefore, remains an open problem. However, we will derive new results for the n -dimensional case under the following assumptions. We only consider the homogeneous case, i.e., all marginal distributions are the same, $F_{X_1} = \dots = F_{X_n} = F_X$. In addition, the distribution function F_X fulfills the following definition.

Definition 2 (*B*-SYM Distribution). Let X_1, \dots, X_n be non-negative continuous random variables with distribution function $F_{X_1} = \dots = F_{X_n} = F_X$ with finite first moment. The distribution function F_X is a *B*-SYM distribution, if the solution to the optimization problem

$$\begin{aligned} s^* &= \min_{(x_1, \dots, x_n)} \sum_{i=1}^n x_i \\ \text{s. t. } &B(x_1, \dots, x_n) = 0 \end{aligned} \quad (16)$$

lies on the identity line, i.e., $s^* = nx^*$ with $B(x^*, \dots, x^*) = 0$.

A characterization of some *B*-SYM distribution functions for two relevant *B* is given in the following lemmas. The two considered *B* in Lemmas 5 and 6 arise from the Fréchet-Hoeffding lower bound and the lower bound on Archimedean copulas [30, Prop. 4.6], respectively. They will later be needed in Theorems 7 and 9 to bound the maximum ZOC.

Lemma 5. For $B(x_1, \dots, x_n) = \sum_{i=1}^n F_X(x_i) - n + 1$, a continuous distributions F_X with a strictly quasi-concave density f_X is a *B*-SYM distribution, if the following sufficient condition holds

$$f'_X \left(F_X^{-1} \left(1 - \frac{1}{n} \right) \right) < 0. \quad (17)$$

Proof. The proof can be found in Appendix C. \square

Lemma 6. For $B(x_1, \dots, x_n) = \sum_{i=1}^n (F_X(x_i))^{\frac{1}{n-1}} - n + 1$, a continuous distribution F_X with a strictly quasi-concave density f_X is a *B*-SYM distribution, if the following two sufficient conditions hold. The function

$$g(x) = \frac{1}{n-1} F_X(x)^{\frac{2-n}{n-1}} f_X(x) \quad (18)$$

is strictly quasi-concave, and

$$\frac{f'_X(x^*)}{(f_X(x^*))^2} < \frac{n-2}{n-1} \left(1 - \frac{1}{n} \right)^{1-n} \quad (19)$$

with

$$x^* = F_X^{-1} \left(\left(1 - \frac{1}{n} \right)^{n-1} \right). \quad (20)$$

Proof. The proof can be found in Appendix D. \square

Remark 3. A stricter condition than (19) is $f'_X(F_X^{-1}(e^{-1})) < 0$. Based on the unimodality of f_X , this can also be written as $F_X(\text{mode}) < e^{-1} \approx 0.368$, where “mode” refers to the mode of distribution F_X . Similarly, we can rewrite (17) as $F_X(\text{mode}) < 1 - \frac{1}{n}$. Since these conditions are stricter than those from the above lemmas, they are also sufficient to characterize a *B*-SYM distribution.

Remark. Note that Lemmas 5 and 6 only present sufficient conditions for *B*-SYM distributions. It is, therefore, possible that other, possibly non-unimodal, distributions exist that are also *B*-SYM.

Remark 4 (Common Fading Distributions). Most of the common fading distributions fulfill the sufficient conditions from Lemmas 5 and 6. In the case of Rayleigh fading, the channel gains X_i are exponentially distributed and therefore have a monotone density, i.e., $f'(x) < 0$ for all x . Other common distributions like log-normal, Gamma, and χ^2 also fulfill the conditions. An example of a distribution that is *not* *B*-SYM for the considered *B*, is a Weibull distribution with scale parameter $\lambda = 1$ and shape parameter $k = 6$ for $n = 2$. For this example, $f'(F^{-1}(0.5)) \approx 1.98 > 0$. The mentioned examples are also illustrated in [28].

1) *Outer Bounds on the Maximum ZOC:* First, we will give two outer bounds on the maximum ZOC. The first one is based on the Fréchet-Hoeffding lower bound W . Even though it is not a valid copula for $n > 2$, the bound from Theorem 2 still holds and can therefore be used as a loose upper bound on the actual maximum ZOC.

Theorem 7 (Outer Bound on the Maximum MRC-ZOC for n Homogeneous Links based on W). Let X_1, \dots, X_n be n non-negative continuous random variables representing the channel gains of n communication channels. All X_i follow the

same distribution, i.e., $F_{X_i} = F_X$ for $i = 1, \dots, n$, which is a B -SYM distribution for $B(x_1, \dots, x_n) = \sum_{i=1}^n F_X(x_i) - n + 1$. The maximum zero-outage capacity R^0 for MRC at the receiver is then upper bounded by

$$\overline{R}_n^0 = \log_2 \left(1 + nF_X^{-1} \left(1 - \frac{1}{n} \right) \right). \quad (21)$$

Proof. The proof can be found in Appendix E. \square

As already mentioned, W is not a copula in the case of $n > 2$. The outer bound from Theorem 7 will therefore be loose. In the following examples in Section IV-C and IV-D, we will see that the gap to the actual maximum ZOC can grow arbitrarily large for large n . A better outer bound can be obtained by using *joint mixability* [31]. Based on [32, Thm. 2.6], a general bound on the best-case ε -outage capacity is derived in [10, Thm. 7]. We will use this to derive an outer bound on the maximum ZOC in the following corollary.

Corollary 8 (Outer Bound on the Maximum MRC-ZOC for n Homogeneous Links based on [10, Thm. 7]). *Let X_1, \dots, X_n be n non-negative continuous random variables representing the channel gains of n communication channels. All X_i follow the same distribution, i.e., $F_{X_i} = F_X$ for $i = 1, \dots, n$. The maximum zero-outage capacity R^0 for MRC at the receiver is then upper bounded by*

$$\overline{R}_n^0 = \log_2 (1 + n\mathbb{E}[X]). \quad (22)$$

Proof. The proof directly follows from [10, Thm. 7]. We only need to set $\varepsilon = 0$ and obtain (22). \square

As stated in [32], the bound is tight, if the distribution F_X is n -completely mixable. Unfortunately, as shown in [31, Rem. 2.2], distributions with a one-sided unbounded support can not be completely mixable. For details on this matter, we refer the readers to [31], [33]. However, as shown in [10], the bound from Corollary 8 might come arbitrarily close to the exact value in some special cases when $n \rightarrow \infty$. We will also observe this behavior for the Rayleigh fading example in Section IV-C.

2) *Inner Bound on the Maximum ZOC:* Next, we derive an inner bound on the maximum ZOC. It is based on the Archimedean copula stated in [30, Prop. 4.6]. Archimedean copulas are a popular class of single-parameter copulas for an arbitrary number of dimensions n . The simple construction for an arbitrary dimension $n > 2$ is one of the reasons for their popularity [13, Chap. 4]. In the following, we need this extension to $n > 2$ and since it is a valid copula, the derived value is achievable and we obtain an inner bound. We use this particular copula since it is a lower bound on all Archimedean copulas [30, Prop. 4.6].

Again, to obtain closed-form solutions, we assume that F_X is a B -SYM distribution. However, with the mentioned copula, an inner bound can also be obtained for arbitrary fading distributions.

Theorem 9 (Inner Bound on the Maximum MRC-ZOC for n Homogeneous Links). *Let X_1, \dots, X_n be n non-negative continuous random variables representing the channel gains of n communication channels. All X_i follow the same distribution,*

i.e., $F_{X_i} = F_X$ for $i = 1, \dots, n$, which is a B -SYM distribution for $B(x_1, \dots, x_n) = \sum_{i=1}^n (F_X(x_i))^{\frac{1}{n-1}} - n + 1$. The maximum zero-outage capacity R^0 for MRC at the receiver is then lower bounded by

$$\underline{R}_n^0 = \log_2 \left(1 + nF_X^{-1} \left(\left(1 - \frac{1}{n} \right)^{n-1} \right) \right). \quad (23)$$

Proof. The proof can be found in Appendix F. \square

3) *Gap Between Inner and Outer Bound:* For distributions that are B -SYM distributions for the boundary function in Theorem 9, we know that the exact value of the maximum ZOC is between the outer bound given in Corollary 8 and the inner bound from Theorem 9. It is therefore of interest to analyze the gap between the bounds. This will be summarized in the following corollary.

Corollary 10 (Maximum Gap between Inner and Outer Bound on the Maximum MRC-ZOC). *Let X_1, \dots, X_n be n non-negative continuous random variables representing the channel gains of n communication channels. All X_i follow the same distribution, i.e., $F_{X_i} = F_X$ for $i = 1, \dots, n$, which is B -SYM for the function B from Theorem 9. The gap between the inner bound on the maximum ZOC from Theorem 9 and the outer bound from Corollary 8 is at most*

$$\overline{R}_n^0 - \underline{R}_n^0 \leq \log_2 \left(\frac{\mathbb{E}[X]}{F_X^{-1}(e^{-1})} \right). \quad (24)$$

Proof. The proof can be found in Appendix G. \square

Corollary 10, therefore, allows us to calculate the maximum ZOC for n homogeneous fading links and MRC at the receiver within a finite amount of bits equal to $\log_2(\mathbb{E}[X]) - \log_2(F_X^{-1}(1/e))$.

C. Example: Rayleigh Fading

In the following, we will illustrate the general results with the example of Rayleigh fading. In this case, all channel gains $|H_i|^2$ are exponentially distributed with mean 1. This gives $\rho_i |H_i|^2 = X_i \sim \exp(1/\rho_i)$. The CDF and inverse CDF of $X_i \sim \exp(\lambda_i)$ are given by

$$F_{X_i}(x) = \begin{cases} 0 & \text{if } x < 0 \\ 1 - \exp(-\lambda_i x) & \text{if } x \geq 0 \end{cases}$$

and

$$F_{X_i}^{-1}(u) = \begin{cases} \frac{-\log(1-u)}{\lambda_i} & \text{if } 0 \leq u < 1 \\ +\infty & \text{if } u = 1, \end{cases}$$

respectively. Note that the expected value of X_i is $1/\lambda_i = \rho_i$.

1) *Two Links:* First, we will take a look at the two-dimensional case. In order to do this, we will evaluate (13) from Theorem 4 in the following.

We start with determining x^* according to (15). This gives the following expression

$$x^*(t) = \frac{-1}{\lambda_1} \log \left(\frac{\lambda_2}{\lambda_1 + \lambda_2} (2 - t) \right).$$

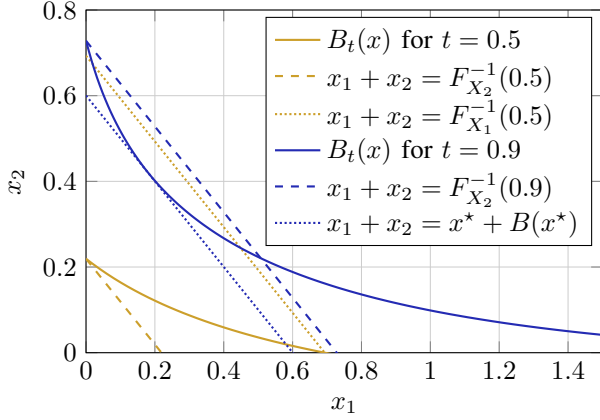


Figure 3. Boundary $B_t(x)$ for Rayleigh fading channels with SNRs $\rho_1 = 0$ dB and $\rho_2 = -5$ dB for the values $t = 0.5$ and $t = 0.9$.

Note that the range of x^* is bounded by 0 and $F_{X_1}^{-1}(t)$. The boundary of \mathcal{B} is computed according to (14) as

$$B_t(x) = -\frac{\log(2 - t - \exp(-\lambda_1 x))}{\lambda_2},$$

and therefore, we get

$$B_t(x^*) = -\frac{\log\left((2-t)\frac{\lambda_1}{\lambda_1+\lambda_2}\right)}{\lambda_2}, \quad (25)$$

when $0 < x^* < F_{X_1}^{-1}(t)$. For the extreme cases, we find that

$$x^* + B(x^*) = \begin{cases} F_{X_2}^{-1}(t) & \text{if } x^* = 0 \\ F_{X_1}^{-1}(t) & \text{if } x^* = F_{X_1}^{-1}(t) \end{cases}.$$

Thus, we can combine the above results according to (13) to get the expression of the ZOC for two Rayleigh fading links as

$$R^0(t) = \log_2\left(1 + x^*(t) - \frac{\log(2 - t - \exp(-\lambda_1 x^*(t)))}{\lambda_2}\right) \quad (26)$$

with

$$x^*(t) = \left[\min\left\{\frac{-1}{\lambda_1} \log\left(\frac{\lambda_2}{\lambda_1 + \lambda_2}(2-t)\right), F_{X_1}^{-1}(t)\right\} \right]^+. \quad (27)$$

Figure 3 shows examples for the function B_t and the possible candidates for $s = 2^{R^0} - 1$. Recall that the idea is to find the line $x_1 + x_2 = s$ with the maximum s such that the line is still below B_t . The different curves are shown for two values of t , namely $t = 0.5$ and $t = 0.9$. It can be seen that the values $F_{X_1}^{-1}(t)$ and $F_{X_2}^{-1}(t)$ increase with increasing t . These are the first candidates for the optimal R^0 from (13). They are represented by the lines $x_1 + x_2 = F_{X_1}^{-1}(t)$ and $x_1 + x_2 = F_{X_2}^{-1}(t)$, respectively. In the case of $t = 0.5$, the optimal s is given by $F_{X_2}^{-1}(0.5)$ since there is no other line of the form $x_1 + x_2 = s$ with a larger s which is still below $B_t(x)$. In contrast, the line $x_1 + x_2 = F_{X_1}^{-1}(t)$ is not below B_t . For the larger value of $t = 0.9$, there exists a tangent point at around $x^* = 0.18$ which gives the maximum $s = 2^{R^0} - 1$ of around 0.6. This can then be used to determine the ZOC R^0 .

The ZOC R^0 from (26) is shown for different values of ρ_1 and ρ_2 in Fig. 4a. As expected, the ZOC increases for increasing SNR values ρ_i , since the channel quality increases. An interesting phenomenon can be seen from the asymmetric constellations of ρ_1 and ρ_2 . Especially, if there is a big difference between them, e.g., $\rho_1 = -5$ dB and $\rho_2 = 10$ dB, the ZOC is low and grows only slowly for small t . However, for larger t , the rate of growth increases. The reason for this is that R^0 is only determined by the weaker channel for small t . This can easily be seen when comparing the case of $\rho_1 = -5$ dB and $\rho_2 = 10$ dB with the case of $\rho_1 = -5$ dB and $\rho_2 = 5$ dB. For t up to around 0.9, both cases achieve the same ZOC R^0 , since their weaker channel has the same SNR of -5 dB. However, for $t > 0.9$, the constellation with the better second channel, i.e., higher ρ_2 , is able to achieve a larger R^0 . The same behavior can be seen for the cases of $\rho_1 = \rho_2 = 0$ dB and $\rho_1 = 0$ dB, $\rho_2 = 5$ dB. The only difference is that the value of t at which the curves start to differ is lower, at around 0.1. This can also be seen from Fig. 4b, where the ZOCs of combinations of ρ_1 and ρ_2 are shown for $t = 0.5$. All of the presented figures are also available as interactive versions at [28]. We encourage the interested readers to change the parameters on their own and explore the behavior of the presented results.

The maximum ZOC is achieved for countermonotonic X_1 and X_2 . This corresponds to a value of $t = 1$. The joint distribution $F_{X,Y}$ in this case is supported on the line

$$x_2 = F_{X_2}^{-1}(1 - F_{X_1}(x_1)) = \frac{-\log(1 - \exp(-\lambda_1 x_1))}{\lambda_2}.$$

From (27), we get $x^*(1) = -\left(\log\frac{\lambda_2}{\lambda_1+\lambda_2}\right)/\lambda_1$ and together with (26) this yields the maximum ZOC

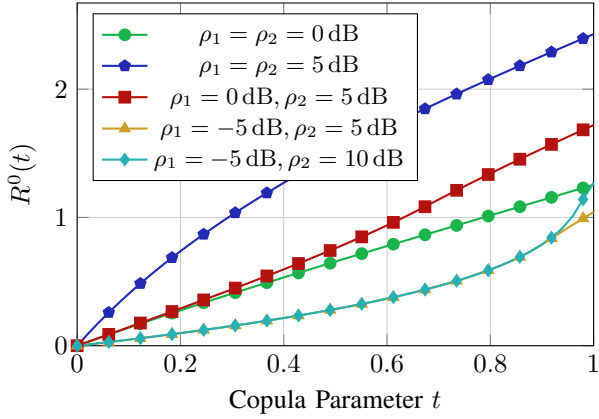
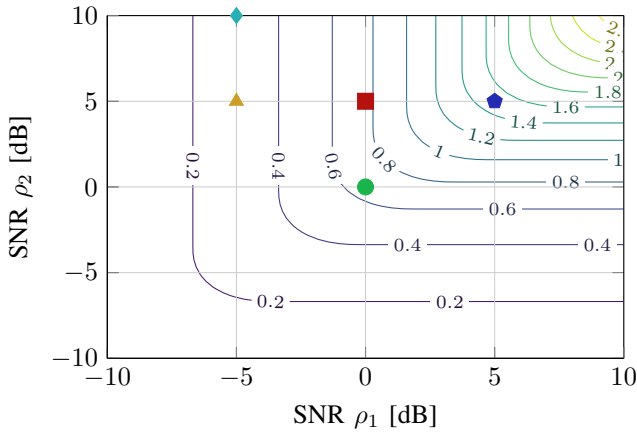
$$R^0(1) = \log_2\left(1 + \frac{\log\frac{\lambda_1+\lambda_2}{\lambda_2}}{\lambda_1} + \frac{\log\frac{\lambda_1+\lambda_2}{\lambda_1}}{\lambda_2}\right). \quad (28)$$

In the case that $\lambda_1 = \lambda_2 = 1$, this evaluates to $R^0(1) = \log_2(1 + 2\log 2)$. The result for this special case was also derived in [9, Thm. 1] and [10, Ex. 3] by different approaches.

2) *General Case:* For the extension to the n -dimensional case, we now assume homogeneous links, i.e., $F_{X_1} = \dots = F_{X_n} = F_X$. We can then apply the results from Section IV-B to find bounds on the maximum ZOC. In addition, if F_X has a strictly monotone density, the exact values for the maximum ZOC are derived in [10]. An example with this property is Rayleigh fading, since the channel gains X_i are exponentially distributed. In the following example, we can therefore compare the exact values from [10] to the bounds from Theorems 7, 9, and Corollary 8 for Rayleigh fading. The results are shown in Fig. 5.

The first upper bound \overline{R}_n^0 , based on the Fréchet-Hoeffding lower bound W , is evaluated according to (21). The second upper bound from Corollary 8 is calculated to

$$\overline{R}_n^0 = \log_2(1 + n\rho). \quad (29)$$

(a) ZOC for different copula parameters t .(b) The copula parameter is set to $t = 0.5$. The marked points correspond to the SNR combinations shown in Fig. 4a.Figure 4. Achievable zero-outage capacities R^0 for two dependent Rayleigh fading channels with different SNR values ρ_1 and ρ_2 . The two channels follow the copula C_t .

As shown in [10], the exact value approaches \overline{R}_n^0 for $n \rightarrow \infty$ in the case of Rayleigh fading. The inner bound from Theorem 9, is evaluated to

$$\underline{R}_n^0 = \log_2 \left(1 - \rho n \log \left(1 - \left(1 - \frac{1}{n} \right)^{n-1} \right) \right). \quad (30)$$

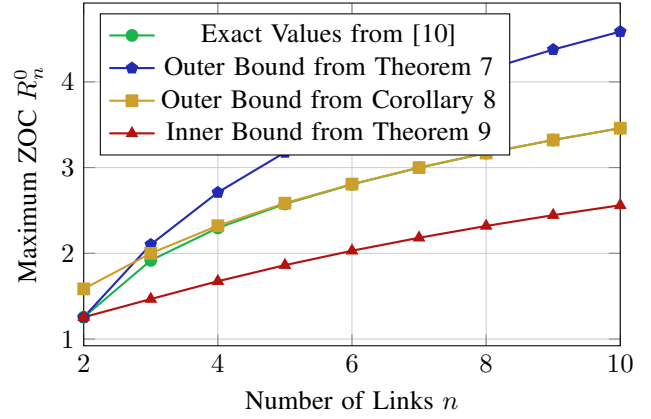
The exact value of the ZOC R_n^0 is between the inner and outer bound, i.e., $\underline{R}_n^0 \leq R_n^0 \leq \overline{R}_n^0$. As described in Corollary 10, the gap between the bounds is upper bounded by

$$\lim_{n \rightarrow \infty} \overline{R}_n^0 - \underline{R}_n^0 = -\log_2(1 - \log(e-1)) \approx 1.12 \text{ bit}. \quad (31)$$

We want to emphasize that the exact values derived in [10] only hold for monotonic densities of the channel gains X_i . It can therefore not be used for all types of fading, e.g., it can not be used for log-normal fading. Therefore the upper and lower bounds derived in the present work are useful and more general.

D. Example: Nakagami- m Fading

We will now give an example of Nakagami- m fading. In this case, $|H_i|$ is distributed according to a Nakagami- m

Figure 5. Exact values and bounds on the maximum ZOC for n Rayleigh fading links with $\rho = 0$ dB.

distribution, i.e., $|H_i| \sim \text{Nakagami}(m, 1)$ [34]. Therefore, the channel gains $X_i = \rho_i |H_i|^2$ are distributed according to a Gamma-distribution, i.e., $X_i \sim \Gamma(m, \rho_i/m)$.

The ZOCs are calculated numerically according to Theorem 4. The source code of the calculations together with interactive versions of the presented figures can be found in [28]. Figure 6 shows $R^0(t)$ for two Nakagami- m fading channels with $m = 5$ for different SNR combinations. As expected, the achievable ZOC increases with increasing SNRs. For asymmetric SNR values ρ_1 and ρ_2 , we can observe a similar behavior compared to the case of Rayleigh fading discussed in the previous section. Up to a certain value of t , the achievable ZOC is only determined by the worse channel. In Fig. 6 this can be seen, e.g., for $\rho_1 = 0$ dB and $\rho_2 = 0$ dB or 5 dB. Up to t around 0.9, both constellations achieve the same ZOC. Above this value, the scenario with the higher ρ_2 achieves higher R^0 . We encourage the interested readers to explore this behavior in the interactive version in [28] with further parameter constellations.

For the homogeneous case with $n > 2$, we select the parameters $m = 5$ and $\rho = 0$ dB. The Gamma distribution with these parameters fulfills the inequality that the mode is less than the median,

$$\text{mode} = \frac{m-1}{m} \rho = 0.8 < \text{median} = 0.934,$$

and we can therefore apply Theorem 7. It is also straightforward to confirm that the distribution fulfills the condition from Lemma 6, which allows us to use Theorem 9. The results for this example are shown in Fig. 7. Similar to the case of Rayleigh fading, the gap between the inner bound \underline{R}_n^0 and the outer bound \overline{R}_n^0 from Theorem 7 grows indefinitely with increasing n . On the other hand, the gap between the inner bound \underline{R}_n^0 and the outer bound \overline{R}_n^0 from Corollary 8 is, according to Corollary 10, always less than around 0.328 bit.

E. Summary

In this section, we showed that there exists an infinite number of joint fading distributions for which the ZOC is positive, if the receiver employs MRC. For the two-dimensional

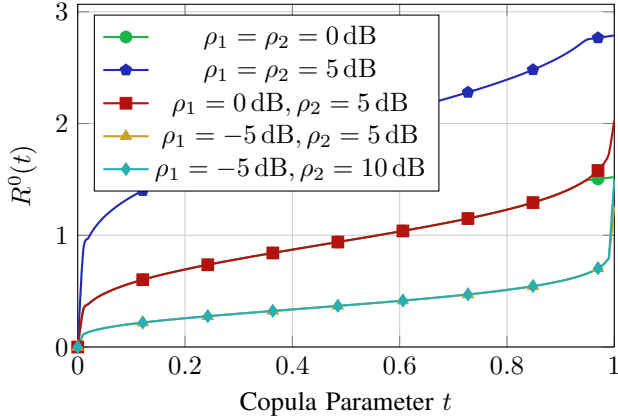


Figure 6. Achievable zero-outage capacities R^0 for two dependent Nakagami- m fading channels with different SNR values ρ_1 and ρ_2 and $m = 5$. The two channels follow the copula C_t defined in Remark 2.

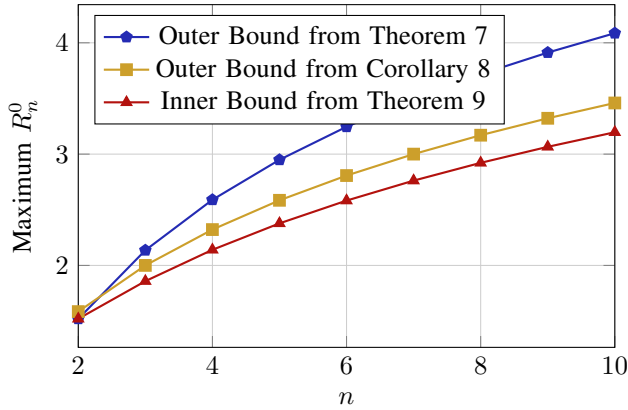


Figure 7. Inner and outer bounds on the maximum ZOC for n Nakagami- m fading links with $m = 5$ and $\rho = 0$ dB.

scenario, we derived a general expression for the maximum ZOC, which can also be applied to heterogeneous marginals. For homogeneous marginals, we extended the results to the case of $n > 2$ under some constraints and provide upper and lower bounds on the maximum ZOC which admit a finite gap. An overview of the results can be found in Table I. The most general scenario of n heterogeneous marginals remains an open problem at this point.

V. SELECTION COMBINING

In this section, we will consider SC as another diversity combining scheme. In this case, only the strongest link is selected at the receiver [35]. The combining function L is therefore given as

$$L_{SC}(X_1, \dots, X_n) = \max\{X_1, \dots, X_n\}.$$

Analogue to Section IV, we start with the two-dimensional case and extend it to the general n -dimensional case. We also evaluate the results for the examples of Rayleigh fading and Nakagami- m fading.

A. Two-Dimensional Case

Similar to MRC, the maximum ZOC for SC with two dimensions is achieved for countermonotonic X_1 and X_2 [36]. The optimization problem (12) can therefore be written as

$$\min_{F_{X_1}(x_1)+F_{X_2}(x_2)=1} \max\{x_1, x_2\}. \quad (32)$$

With the substitutions $x_1 = F_{X_1}^{-1}(p)$ and $x_2 = F_{X_2}^{-1}(1-p)$, we rewrite the problem as

$$\min_{p \in [0,1]} \max\{F_{X_1}^{-1}(p), F_{X_2}^{-1}(1-p)\}. \quad (33)$$

Recall that the quantile function F_X^{-1} is an increasing function. Combined with the assumption that all X_i are supported on the non-negative real numbers, we can derive that the minimum is attained at p^* for which

$$F_{X_1}^{-1}(p^*) = F_{X_2}^{-1}(1-p^*) \quad (34)$$

holds. The maximum ZOC is then given as

$$R^0 = \log_2(1 + F_{X_1}^{-1}(p^*)). \quad (35)$$

In the case of homogeneous marginals, i.e., $F_{X_1} = F_{X_2} = F_X$, we get $p^* = 0.5$. The ZOC from (35) can then be simplified to $R^0 = \log_2(1 + \text{median}(X))$.

B. General Case

For the extension to the n -dimensional case, first, recall the general problem formulation from (3). We are interested in the case that the outage probability is zero, i.e., $\Pr(L(X_1, \dots, X_n) < s) = 0$.

For homogeneous marginals $F_{X_1} = \dots = F_{X_n} = F_X$, we determine the exact solution to (3) as follows. From [37], we know that there always exists a *maximally dependent* coupling of (X_1, \dots, X_n) such that

$$\Pr\left(\max(X_1, \dots, X_n) < F_X^{-1}\left(1 - \frac{1}{n}\right)\right) = 0, \quad (36)$$

if all X_i are identically distributed. This can now be used to solve the optimization problem (3) and find the maximum ZOC for SC at the receiver as

$$R_n^0 = \log_2\left(1 + F_X^{-1}\left(1 - \frac{1}{n}\right)\right). \quad (37)$$

In order to extend the above to the general n -dimensional case with heterogeneous marginal distributions, we leverage the results derived in [38]. With [38, Thm. 7], we derive the implicit characterization of the maximum ZOC R_n^0 for SC as

$$\sum_{i=1}^n F_{X_i}\left(2^{R_n^0} - 1\right) = n - 1, \quad (38)$$

where F_{X_i} corresponds to marginal distributions of X_i , i.e., $X_i \sim F_{X_i}$. Note that this is consistent with the result from (37) for homogeneous marginals, i.e., when $F_{X_1} = \dots = F_{X_n} = F_X$.

Table I
 MAXIMUM ZOC FOR MAXIMUM RATIO COMBINING $L_{\text{MRC}}(X_1, \dots, X_n) = \sum_{i=1}^n X_i$

	Homogeneous Links		Heterogeneous Links
	<i>B</i> -SYM Distribution	General	
$n = 2$	$\log_2(1 + 2 \text{median}(X))$	See Heterogeneous Links	$\log_2(1 + x^* + F_{X_2}^{-1}(1 - F_{X_1}(x^*)))$
$n > 2$	$\overline{R_n^0} - \underline{R_n^0} \leq \log_2\left(\frac{\mathbb{E}[X]}{F_X^{-1}\left(\frac{1}{e}\right)}\right)$	Open Problem	Open Problem

C. Examples

We will now evaluate the results for SC at the receiver for Rayleigh fading and Nakagami- m fading. The first example is for two heterogeneous links. The first link is Rayleigh fading, i.e., $X_1 \sim \exp(1/\rho_1)$, while the second is Nakagami- m fading, i.e., $X_2 \sim \Gamma(m, \rho_2/m)$. The parameters are set to $m = 5$ and $\rho_1 = \rho_2 = 10$ dB. The maximum ZOC is evaluated according to (35), which yields $p^* = 0.575$, $s_{\text{SC}}^* = 8.554$, and $R^0 = 3.256$.

Next, we consider the homogeneous case with $n \geq 2$. In this case, the maximum ZOC is given by (37). For Rayleigh fading, we get

$$R_n^0 = \log_2(1 + \rho \log n), \quad (39)$$

and for Nakagami- m fading, we get

$$R_n^0 = \log_2\left(1 + \frac{\rho}{m} P^{-1}\left(m, 1 - \frac{1}{n}\right)\right), \quad (40)$$

where $P^{-1}(a, z)$ is the inverse of the regularized lower incomplete Gamma function $P(a, z)$ [39, Eq. 6.5.1]. The maximum ZOCs for these fading types are shown in Fig. 8. First, recall that Rayleigh fading is a special case of Nakagami- m fading. It is achieved by setting $m = 1$. From Fig. 8, it can be seen that the maximum ZOC increases for all fading distributions with increasing n . However, the maximum ZOC increases slower for higher m . This is due to the shape of the Gamma-distribution. For increasing m , the probability mass in the upper tail gets smaller. The changes in the quantile function F_X^{-1} are therefore very small, if we look at probabilities close to one, which is the case for $1 - 1/n$ with increasing n . Therefore the changes in the maximum ZOC are also small when m is high. However, it should be emphasized that the maximum ZOC still goes to infinity for $n \rightarrow \infty$. On the other hand, the median increases with increasing m and the maximum ZOC therefore also increases with m for $n = 2$.

D. Summary

In this section, we derived expressions for the maximum ZOC, if the receiver employs SC. An overview of the results can be found in Table II. For homogeneous marginals, we derived the maximum ZOC explicitly for all $n \geq 2$. For n heterogeneous marginals, we give an implicit characterization of the maximum ZOC.

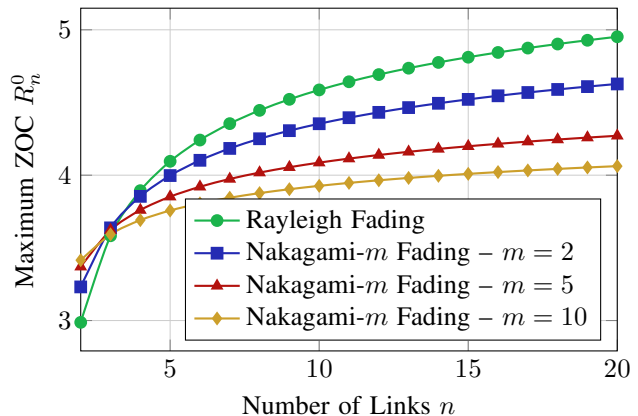


Figure 8. Maximum ZOC for n links with Rayleigh and Nakagami- m fading with SNR $\rho = 10$ dB and SC at the receiver.

Table II
 MAXIMUM ZOC FOR SELECTION COMBINING
 $L_{\text{SC}}(X_1, \dots, X_n) = \max(X_1, \dots, X_n)$

	Homogeneous Links	Heterogeneous Links
	$n = 2$	$\log_2\left(1 + F_X^{-1}\left(1 - \frac{1}{n}\right)\right)$
$n > 2$	$\log_2\left(1 + F_X^{-1}\left(1 - \frac{1}{n}\right)\right)$	$\sum_{i=1}^n F_{X_i}(2^{R_n^0} - 1) = n - 1$

VI. CONCLUSION

In this work, we investigated the ZOC for fading channels with a dependency structure. Interestingly, there exist joint distributions for which the ZOC is strictly positive, without requiring perfect CSI-T, i.e., without power control and only with an average power constraint. First, we provide a parameterized description of a dependency structure in form of a copula that achieves positive ZOCs. This shows that the set of joint distribution, for which the ZOC is positive, is not a singleton. Next, we investigated the maximum ZOC over all joint distributions with given marginals. In the homogeneous case, i.e., all marginal distributions are the same, we provide an explicit expression for the maximum ZOC when SC is used at the receiver as diversity combining technique. For MRC at the receiver, we derive upper and lower bounds on the maximum ZOC. The gap between these bounds is finite for marginal distributions that fulfill certain mild requirements. For heterogeneous marginals, we describe the solution in the case of $n = 2$. The general n -dimensional case with heterogeneous marginal distributions remains an open problem.

at this moment.

This work gives a theoretical analysis and shows how dependency control among random variables can enable ultra-reliable communications, which is of particular interest for URLLC. In future work, it will be necessary to address ways of implementing active dependency control in real communication systems. Key technologies enabling this might be smart relaying [29] or RISs [12]. If a future technology allows a flexible tuning of the radio environment, it might also be interesting to relax the constraint of fixed marginals. Furthermore, we will consider different forms of available CSI at the transmitter in future work.

APPENDIX A PROOF OF COROLLARY 3

It follows from [36, Thm. 3.2] that for a given rate, the lowest-possible outage probability ε is achieved for a joint distribution following the copula [36, Eq. (3.4)]

$$C_\varepsilon(a, b) = \begin{cases} \max[a + b - 1, \varepsilon] & \text{if } (a, b) \in [\varepsilon, 1]^2 \\ M(a, b) & \text{otherwise.} \end{cases} \quad (41)$$

For some further details also see [23], [40]. This dependency structure, therefore, describes the upper bound on the ε -outage capacity for dependent fading channels. Since we are interested in the maximum *zero*-outage capacity, we set $\varepsilon = 0$ and get $C_0(a, b) = W(a, b)$, i.e., the Fréchet-Hoeffding lower bound, as optimal dependency structure.

APPENDIX B PROOF OF THEOREM 4

Let the joint distribution of X_1 and X_2 be determined by the copula

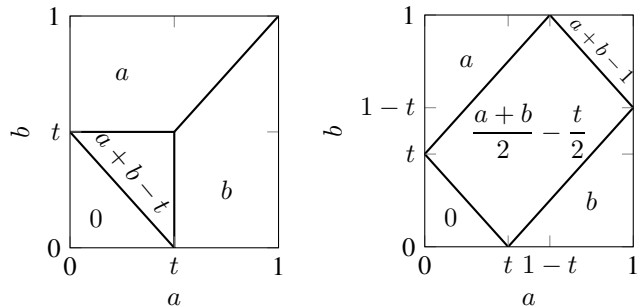
$$C_t(a, b) = \begin{cases} \max[a + b - t, 0] & \text{if } (a, b) \in [0, t]^2 \\ M(a, b) & \text{otherwise} \end{cases} \quad (42)$$

with $t \in [0, 1]$. The copula is also shown in Fig. 9a. For $t = 0$ and $t = 1$, C_t is equal to the Fréchet-Hoeffding upper and lower bounds, respectively. Observe that $C_t(a, b) = 0$ if $a + b \leq t$. Since we are interested in the area \mathcal{S} , cf. (10), we need to transform the area from the copula space into the space of x_1 and x_2 . From Sklar's theorem, we know that $F_{X_1, X_2}(x, y) = 0$, if $F_{X_1}(x_1) + F_{X_2}(x_2) \leq t$. We will refer to this area as \mathcal{B} as defined in (11) in the following.

We denote the boundary of \mathcal{B} as $B_t(x) = F_{X_2}^{-1}(t - F_{X_1}(x))$. Since we are looking for a tangent with slope -1 , we have the following condition

$$\frac{\partial B_t}{\partial x_1} = \frac{-f_{X_1}(x)}{f_{X_2}(F_{X_2}^{-1}(t - F_{X_1}(x)))} \stackrel{!}{=} -1, \quad (43)$$

where we set $u = t - F_{X_1}(x_1)$ and apply the well-known rules for derivatives. The solutions to (43) are denoted as $x^{(i)}$. Recall that we are looking for lines in the form of $x_1 + x_2 = s$ and that the above condition gives these tangents on B at $x^{(i)}$. The next candidate solutions are therefore in the form $x_1 + x_2 = x^{(i)} + B_t(x^{(i)})$. An exemplary \mathcal{B} can be seen in Fig. 10. It is easy to see that there exist



(a) Copula from [13, Chap. 3.2.2] (b) Generalized Circular Copula

Figure 9. Two different copulas with parameter t which allow achieving a positive ZOC.

multiple solutions $x^{(i)}$ to (43). However, only one of the lines $x^{(i)} + B(x^{(i)})$ lies completely in \mathcal{B} . For the optimal solution x^* , we, therefore, need to take the minimum over all $x^{(i)}$, i.e., $x^* = \arg \min_{x^{(i)}} \{x^{(i)} + B(x^{(i)})\}$.

If the boundary \mathcal{B} is not convex or it has no slope of -1 in the first quadrant of the x_1 - x_2 plane, we need to consider the limit points, which are given at $x_1 = 0$ and $x_2 = 0$ and we have $x_2 \leq F_{X_2}^{-1}(t)$ and $x_1 \leq F_{X_1}^{-1}(t)$, respectively. Recall that the original problem $x_1 + x_2 \leq s$ can be viewed as finding the line $x_2 = s - x_1$ with the maximum s such that the line is in \mathcal{B} . With the first bounds on x_1 and x_2 , we have the simple lines $x_1 + x_2 = F_{X_1}^{-1}(t)$ and $x_1 + x_2 = F_{X_2}^{-1}(t)$ as possible candidates. This is illustrated in Fig. 10. From this exemplary plot, it is also easy to see that both lines do not fully lie in \mathcal{B} . Thus, there is a positive probability mass in the areas $x_1 + x_2 \leq F_{X_1}^{-1}(t)$ and $x_1 + x_2 \leq F_{X_2}^{-1}(t)$. In this case, we need to find the tangent on the boundary of \mathcal{B} . We now have the following possible candidates for s

$$s_1 = x^* + B_t(x^*), \quad s_2 = F_{X_1}^{-1}(t), \quad s_3 = F_{X_2}^{-1}(t).$$

Recall that $s = 2^{R^0} - 1$ with the ZOC R^0 when the joint distribution of X_1 and X_2 follow copula C_t . With reference to Fig. 10, it becomes clear that we need to take the minimum of all s_i in order to guarantee that $x_1 + x_2 \leq s$ is a subset of \mathcal{B} . Combining all of the above finally states the theorem.

APPENDIX C PROOF OF LEMMA 5

We start with the following observation. Since we want to minimize the sum $\sum_{i=1}^n x_i$, we are interested in the tangent planes $\sum_{i=1}^n x_i = s$ on $B(\mathbf{x}) = 0$. The condition for the critical points is therefore given by

$$\frac{\partial B}{\partial x_i} = \frac{\partial B}{\partial x_j}, \quad \forall i, j. \quad (44)$$

For the considered B , this means that

$$f(x_i) = f(x_j), \quad \forall i, j. \quad (45)$$

First, it is easy to see from this, that there will always be a critical point on the identity line $x_1 = \dots = x_n$ that solves (45). If the density f is strictly decreasing, e.g., the exponential distribution, it has an inverse function and the

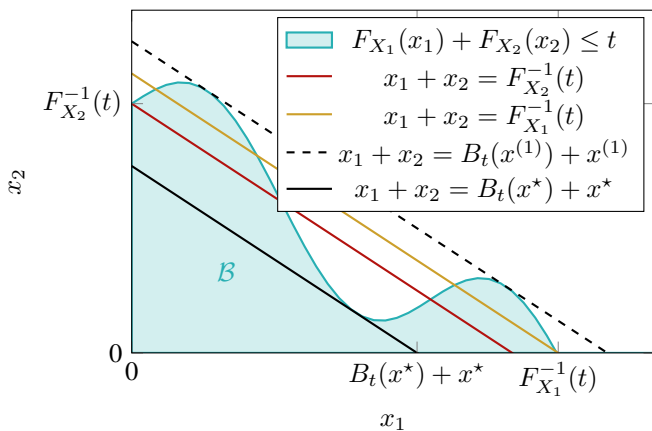


Figure 10. Area with zero probability mass of the joint distribution F_{X_1, X_2} and different candidates for corresponding ZOC.

point on the identity line will be the only solution (45). For such distributions, the proof is concluded.

For general distributions with quasiconcave densities, we next check the curvature of B at the point on the identity line that we are interested in. If it is negative, this corresponds to a maximum of the curve and is *not* a solution of (16). If we have a minimum on the identity line, it is a valid candidate to be the solution to (16).

With the implicit function theorem [41, Sec. 8.3], we will express the implicit function $B(x_1, \dots, x_n) = 0$ by an explicit function $b(x_1, \dots, x_{n-1})$ as

$$B(x_1, \dots, x_n) = 0 \Leftrightarrow b(x_1, \dots, x_{n-1}) = x_n. \quad (46)$$

From the implicit function theorem, we can determine the gradient of b as

$$\frac{\partial b}{\partial x_i} = - \left(\frac{\partial B}{\partial x_n} \right)^{-1} \frac{\partial B}{\partial x_i}, \quad i = 1, \dots, n-1, \quad (47)$$

and the second derivatives, i.e., the Hessian matrix, whose entries are then given by

$$\frac{\partial^2 b}{\partial x_i \partial x_j} = - \left(\frac{\partial B}{\partial x_n} \right)^{-2} \left(\frac{\partial^2 B}{\partial x_i \partial x_j \partial x_n} \frac{\partial B}{\partial x_n} - \frac{\partial B}{\partial x_i} \frac{\partial^2 B}{\partial x_n \partial x_j} \right). \quad (48)$$

For the considered B , this gives

$$\frac{\partial^2 b}{\partial x_i^2} = - \frac{f'(x_i)}{f(x_n)} \quad (49)$$

and

$$\frac{\partial^2 b}{\partial x_i \partial x_j} = 0, \quad i \neq j, \quad (50)$$

where f' is the derivative of the density. From this, it can be seen that the Hessian matrix of B is a diagonal matrix and its eigenvalues are therefore the entries on the main diagonal which are given by (49). In order to have a minimum on the identity line, the Hessian needs to be positive definite at this point, i.e., all of its eigenvalues need to be positive. From (49), we see that this is the case if

$$f'(x^*) = f' \left(F^{-1} \left(1 - \frac{1}{n} \right) \right) < 0, \quad (51)$$

which is exactly (17).

We have shown that there is a local minimum on the identity line for distributions that fulfill the above condition, and we now show that this is then also a global minimum. For this, recall that all other critical points are given by (45). For the general case of a strictly quasiconcave density, we know that there are two solutions to $f(x) = \alpha$ for each level set α , due to the unimodality. One of the solutions is greater than the mode while the other is less than the mode. If all x_i are on the same side from the mode, they are all equal and this is, therefore, the point on the identity line that we already considered. We, therefore, have to check the remaining solutions, i.e., when at least two x_i are on the different sides of the mode. In this case, the x_i that is less than the mode is on the increasing part of the density, i.e., $f'(x_i) > 0$, while $f'(x_j) < 0$, when x_j is greater than the mode. With (49), we can therefore conclude that the Hessian matrix is indefinite at all remaining critical points, i.e., they are saddle points.

Since we assume unbounded support of F_X , the range of each x_i is $[0, \infty)$. Therefore, if $x_i \rightarrow \infty$ for any i , the sum $x_1 + \dots + x_n$ also tends to ∞ . In other words, the function is coercive [42, Def. 2.31] with respect to the sum.

We can summarize the above discussion as follows. A distribution that fulfills condition (17) from the lemma has a unique minimum of the sum on the identity line. All other stationary points are saddle points. Combining this with the coerciveness, we can conclude that the minimum on the identity line is global.

APPENDIX D PROOF OF LEMMA 6

The proof of Lemma 6 follows the same idea as the proof of Lemma 5. However, we now consider $B(x_1, \dots, x_n) = \sum_{i=1}^n (F_X(x_i))^{\frac{1}{n-1}} - n + 1$. The first derivatives of B are given as

$$\frac{\partial B}{\partial x_i} = g(x_i) = \frac{1}{n-1} (F(x_i))^{\frac{2-n}{n-1}} f(x_i). \quad (52)$$

Thus, the critical points for the tangent plane are now given by the condition

$$(F(x_i))^{\frac{2-n}{n-1}} f(x_i) = (F(x_j))^{\frac{2-n}{n-1}} f(x_j), \quad \forall i, j. \quad (53)$$

The second partial derivatives of B are given as

$$\frac{\partial^2 B}{\partial x_i^2} = g'(x_i) = \frac{(F(x_i))^{\frac{2-n}{n-1}}}{n-1} \left(f'(x_i) + \frac{2-n}{n-1} \frac{(f(x_i))^2}{F(x_i)} \right) \quad (54)$$

and

$$\frac{\partial^2 B}{\partial x_i \partial x_j} = 0, \quad i \neq j. \quad (55)$$

Combining this with (48), we can see that the Hessian matrix again is a diagonal matrix, where the entries on the main diagonal are given by (54). Similarly to the proof of Lemma 5, we have a minimum on the identity line, if the Hessian matrix is positive definite at this point. From the condition $B(x_1, \dots, x_n) = 0$, we get the point on the identity line as

$$x_1 = \dots = x_n = x^* = F^{-1} \left(\left(1 - \frac{1}{n} \right)^{n-1} \right).$$

All of the eigenvalues of the Hessian are positive if

$$f'(x^*) < -\frac{2-n}{n-1} \left(1 - \frac{1}{n}\right)^{1-n} f(x^*)^2. \quad (56)$$

This is condition (19) from the lemma to prove.

By the assumption in the lemma, $g(x)$ is a unimodal function. We can therefore use the same argument as in the proof of Lemma 5 in App. C. With the above observations and reference to App. C, this concludes the proof.

APPENDIX E PROOF OF THEOREM 7

The general idea of the proof is similar to the one of Theorem 4 for two links. However, we need to do the following adjustments. Recall that we want to find the hyperplane of the form

$$\sum_{i=1}^n x_i = s, \quad (57)$$

which touches \mathcal{B} given by $\sum_{i=1}^n F_{X_i}(x_i) + 1 - n = 0$. Since we assume that the distribution is B -SYM, we know this tangent point x^* will be on the identity line, i.e., $x^* = x_1 = \dots = x_n$. We therefore get $x^* = F_X^{-1}\left(\frac{n-1}{n}\right)$, and applying this to (57) gives the corresponding s^* as $s^* = nx^* = nF_X^{-1}\left(\frac{n-1}{n}\right)$. With the definition of s , we get the statement (21) from the theorem.

APPENDIX F PROOF OF THEOREM 9

The proof is basically the same as the one of Theorem 7. The only difference is that we use the lower bound on the Archimedean copulas [30, Prop. 4.6] (also see [43, Prop. 2])

$$C_n(u_1, \dots, u_n) = \left(\left[\sum_{i=1}^n u_i^{\frac{1}{n-1}} - n + 1 \right]^+ \right)^{n-1}.$$

Since this is a valid copula, the derived bound in (23) is achievable and therefore an inner bound on the maximum ZOC.

APPENDIX G PROOF OF COROLLARY 10

The difference of \overline{R}_n^0 in (22) and \underline{R}_n^0 in (23) can be written as

$$\overline{R}_n^0 - \underline{R}_n^0 = \log_2 \left(\frac{1 + n\mathbb{E}[X]}{1 + nF_X^{-1}\left(\left(1 - \frac{1}{n}\right)^{n-1}\right)} \right).$$

The gap increases with increasing n and is therefore upper bounded by

$$\lim_{n \rightarrow \infty} \overline{R}_n^0 - \underline{R}_n^0 = \log_2 \left(\frac{\mathbb{E}[X]}{F_X^{-1}\left(\frac{1}{e}\right)} \right),$$

which is (24).

REFERENCES

- [1] K.-L. Besser, P.-H. Lin, and E. A. Jorswieck, "On the set of joint Rayleigh fading distributions achieving positive zero-outage capacities," in *2020 54th Asilomar Conference on Signals, Systems, and Computers*, IEEE, Nov. 2020, pp. 882–886. DOI: [10.1109/IEEECONF51394.2020.9443271](https://doi.org/10.1109/IEEECONF51394.2020.9443271).
- [2] W. Saad, M. Bennis, and M. Chen, "A vision of 6G wireless systems: Applications, trends, technologies, and open research problems," *IEEE Network*, pp. 1–9, 2019. DOI: [10.1109/mnet.001.1900287](https://doi.org/10.1109/mnet.001.1900287).
- [3] J. Park, S. Samarakoon, H. Shiri, M. K. Abdel-Aziz, T. Nishio, A. Elgabri, and M. Bennis, *Extreme URLLC: Vision, challenges, and key enablers*, Jan. 2020. arXiv: [2001.09683](https://arxiv.org/abs/2001.09683) [cs.IT].
- [4] M. Bennis, M. Debbah, and H. V. Poor, "Ultrareliable and low-latency wireless communication: Tail, risk, and scale," *Proceedings of the IEEE*, vol. 106, no. 10, pp. 1834–1853, Oct. 2018. DOI: [10.1109/JPROC.2018.2867029](https://doi.org/10.1109/JPROC.2018.2867029).
- [5] J. Ding, M. Nemat, S. Pokhrel, O.-S. Park, J. Choi, and F. Adachi, "Enabling grant-free URLLC: An overview of principle and enhancements by massive MIMO," *TechRxiv*, May 2021. DOI: [10.36227/techrxiv.14498505.v1](https://doi.org/10.36227/techrxiv.14498505.v1).
- [6] D. Tse and P. Viswanath, *Fundamentals of Wireless Communications*. Cambridge University Press, 2005.
- [7] B. Zhu and J. Cheng, "Asymptotic outage analysis on dual-branch diversity receptions over non-identically distributed correlated lognormal channels," *IEEE Transactions on Communications*, vol. 67, no. 10, pp. 7126–7138, Oct. 2019. DOI: [10.1109/tcomm.2019.2924882](https://doi.org/10.1109/tcomm.2019.2924882).
- [8] B. Zhu, J. Cheng, J. Yan, J.-y. Wang, L. Wu, and Y. Wang, "A new asymptotic analysis technique for diversity receptions over correlated lognormal fading channels," *IEEE Transactions on Communications*, vol. 66, no. 2, pp. 845–861, Feb. 2018. DOI: [10.1109/TCOMM.2017.2767039](https://doi.org/10.1109/TCOMM.2017.2767039). arXiv: [1707.08200](https://arxiv.org/abs/1707.08200) [cs.IT].
- [9] E. Jorswieck and P.-H. Lin, "Ultra-reliable multi-connectivity with negatively dependent fading channels," in *2019 16th International Symposium on Wireless Communication Systems (ISWCS)*, IEEE, Aug. 2019, pp. 373–378. DOI: [10.1109/ISWCS.2019.8877179](https://doi.org/10.1109/ISWCS.2019.8877179).
- [10] K.-L. Besser and E. A. Jorswieck, "Reliability bounds for dependent fading wireless channels," *IEEE Transactions on Wireless Communications*, vol. 19, no. 9, pp. 5833–5845, Sep. 2020. DOI: [10.1109/TWC.2020.2997332](https://doi.org/10.1109/TWC.2020.2997332). arXiv: [1909.01415](https://arxiv.org/abs/1909.01415) [cs.IT].
- [11] H. Tataria, M. Shafi, A. F. Molisch, M. Dohler, H. Sjoland, and F. Tufvesson, "6G wireless systems: Vision, requirements, challenges, insights, and opportunities," *Proceedings of the IEEE*, vol. 109, no. 7, pp. 1166–1199, Jul. 2021. DOI: [10.1109/jproc.2021.3061701](https://doi.org/10.1109/jproc.2021.3061701).
- [12] M. Di Renzo, M. Debbah, D.-T. Phan-Huy, A. Zappone, M.-S. Alouini, C. Yuen, V. Sciancalepore, G. C. Alexandropoulos, J. Hoydis, H. Gacanin, J. de Rosny, A. Bounceur, G. Lerosey, and M. Fink, "Smart radio environments empowered by reconfigurable AI meta-surfaces: An idea whose time has come," *EURASIP Journal on Wireless Communications and Networking*, vol. 2019, no. 1, p. 129, Dec. 2019. DOI: [10.1186/s13638-019-1438-9](https://doi.org/10.1186/s13638-019-1438-9).
- [13] R. B. Nelsen, *An Introduction to Copulas*, 2nd ed., ser. Springer Series in Statistics. Springer New York, 2006. DOI: [10.1007/0-387-28678-0](https://doi.org/10.1007/0-387-28678-0).
- [14] J. A. Ritcey, "Copula models for wireless fading and their impact on wireless diversity combining," in *2007 Conference Record of the Forty-First Asilomar Conference on Signals, Systems and Computers*, IEEE, Nov. 2007, pp. 1564–1567. DOI: [10.1109/ACSSC.2007.4487493](https://doi.org/10.1109/ACSSC.2007.4487493).
- [15] J. Kitchen and W. Moran, "Copula techniques in wireless communications," *ANZIAM Journal*, vol. 51, pp. 526–540, Aug. 2010. DOI: [10.21914/anziamj.v51i0.2451](https://doi.org/10.21914/anziamj.v51i0.2451).
- [16] M. H. Gholizadeh, H. Amindavar, and J. A. Ritcey, "On the capacity of MIMO correlated Nakagami- m fading channels using copula," *EURASIP Journal on Wireless Communications and Networking*, vol. 2015, no. 1, p. 138, Dec. 2015. DOI: [10.1186/s13638-015-0369-3](https://doi.org/10.1186/s13638-015-0369-3).
- [17] G. W. Peters, T. A. Myrvoll, T. Matsui, I. Nevat, and F. Septier, "Communications meets copula modeling: Non-standard dependence features in wireless fading channels," in *2014 IEEE Global Conference on Signal and Information Processing (GlobalSIP)*, IEEE, Dec. 2014, pp. 1224–1228. DOI: [10.1109/GlobalSIP.2014.7032317](https://doi.org/10.1109/GlobalSIP.2014.7032317).
- [18] F. R. Ghadi and G. A. Hodtani, "Copula function-based analysis of outage probability and coverage region for wireless multiple access communications with correlated fading channels," *IET Communications*, vol. 14, no. 11, pp. 1804–1810, Jul. 2020. DOI: [10.1049/iet-com.2019.0830](https://doi.org/10.1049/iet-com.2019.0830).
- [19] C. Zheng, M. Egan, L. Clavier, G. W. Peters, and J.-M. Gorce, "Copula-based interference models for IoT wireless networks," in *ICC 2019 –*

- 2019 *IEEE International Conference on Communications (ICC)*, IEEE, May 2019. DOI: [10.1109/ICC.2019.8761783](https://doi.org/10.1109/ICC.2019.8761783).
- [20] K.-L. Besser and E. A. Jorswieck, "Bounds on the secrecy outage probability for dependent fading channels," *IEEE Transactions on Communications*, vol. 69, no. 1, pp. 443–456, Jan. 2021. DOI: [10.1109/TCOMM.2020.3026654](https://doi.org/10.1109/TCOMM.2020.3026654). arXiv: [2004.06644](https://arxiv.org/abs/2004.06644) [cs.IT].
- [21] K.-L. Besser and E. A. Jorswieck, "Bounds on the ergodic secret-key capacity for dependent fading channels," in *2020 International ITG Workshop on Smart Antennas (WSA)*, VDE, Feb. 2020.
- [22] F. R. Ghadi and G. A. Hodtani, "Copula-based analysis of physical layer security performances over correlated Rayleigh fading channels," *IEEE Transactions on Information Forensics and Security*, vol. 16, pp. 431–440, 2021. DOI: [10.1109/TIFS.2020.3014553](https://doi.org/10.1109/TIFS.2020.3014553).
- [23] K.-L. Besser and E. A. Jorswieck, "Copula-based bounds for multi-user communications – Part II: Outage Performance," *IEEE Communications Letters*, vol. 25, no. 1, pp. 8–12, 2021. DOI: [10.1109/LCOMM.2020.3023050](https://doi.org/10.1109/LCOMM.2020.3023050). arXiv: [2009.09886](https://arxiv.org/abs/2009.09886) [cs.IT].
- [24] E. A. Jorswieck and K.-L. Besser, "Copula-based bounds for multi-user communications – Part I: Average Performance," *IEEE Communications Letters*, vol. 25, no. 1, pp. 3–7, 2021. DOI: [10.1109/LCOMM.2020.3023056](https://doi.org/10.1109/LCOMM.2020.3023056). arXiv: [2009.09852](https://arxiv.org/abs/2009.09852) [cs.IT].
- [25] P.-H. Lin, E. A. Jorswieck, R. F. Schaefer, C. R. Janda, and M. Mittelbach, "Copulas and multi-user channel orders," in *ICC 2019 – 2019 IEEE International Conference on Communications (ICC)*, IEEE, May 2019. DOI: [10.1109/icc.2019.8761813](https://doi.org/10.1109/icc.2019.8761813).
- [26] P.-H. Lin, E. A. Jorswieck, C. R. Janda, M. Mittelbach, and R. F. Schaefer, "On stochastic orders and fading Gaussian multi-user channels with statistical CSIT," in *2019 IEEE International Symposium on Information Theory (ISIT)*, IEEE, Jul. 2019. DOI: [10.1109/isit.2019.8849386](https://doi.org/10.1109/isit.2019.8849386).
- [27] P.-H. Lin, E. A. Jorswieck, R. F. Schaefer, M. Mittelbach, and C. R. Janda, "New capacity results for fading Gaussian multiuser channels with statistical CSIT," *IEEE Transactions on Communications*, vol. 68, no. 11, pp. 6761–6774, 2020. DOI: [10.1109/tcomm.2020.3013614](https://doi.org/10.1109/tcomm.2020.3013614).
- [28] K.-L. Besser. (2021). "Set of joint distributions achieving positive zero-outage capacities, Supplementary material." [Online]. Available: <https://gitlab.com/klb2/zero-outage-joint-distributions>.
- [29] T. Wang, G. Giannakis, and R. Wang, "Smart regenerative relays for link-adaptive cooperative communications," *IEEE Transactions on Communications*, vol. 56, no. 11, pp. 1950–1960, Nov. 2008. DOI: [10.1109/TCOMM.2008.060688](https://doi.org/10.1109/TCOMM.2008.060688).
- [30] A. J. McNeil and J. Nešlehová, "Multivariate Archimedean copulas, d -monotone functions and ℓ_1 -norm symmetric distributions," *Annals of Statistics*, vol. 37, no. 5B, pp. 3059–3097, Oct. 2009. DOI: [10.1214/07-AOS556](https://doi.org/10.1214/07-AOS556). arXiv: [0908.3750](https://arxiv.org/abs/0908.3750) [math.ST].
- [31] B. Wang and R. Wang, "Joint mixability," *Mathematics of Operations Research*, vol. 41, no. 3, pp. 808–826, Aug. 2016. DOI: [10.1287/moor.2015.0755](https://doi.org/10.1287/moor.2015.0755). SSRN: <https://ssrn.com/abstract=2557067>.
- [32] R. Wang, L. Peng, and J. Yang, "Bounds for the sum of dependent risks and worst value-at-risk with monotone marginal densities," *Finance and Stochastics*, vol. 17, no. 2, pp. 395–417, Apr. 2013. DOI: [10.1007/s00780-012-0200-5](https://doi.org/10.1007/s00780-012-0200-5).
- [33] G. Puccetti, B. Wang, and R. Wang, "Advances in complete mixability," *Journal of Applied Probability*, vol. 49, no. 2, pp. 430–440, Jun. 2012. DOI: [10.1239/jap/1339878796](https://doi.org/10.1239/jap/1339878796).
- [34] M. D. Yacoub, "The α - μ distribution: A general fading distribution," in *The 13th IEEE International Symposium on Personal, Indoor and Mobile Radio Communications*, IEEE, 2002, pp. 629–633. DOI: [10.1109/PIMRC.2002.1047298](https://doi.org/10.1109/PIMRC.2002.1047298).
- [35] D. Brennan, "Linear diversity combining techniques," *Proceedings of the IRE*, vol. 47, no. 6, pp. 1075–1102, Jun. 1959. DOI: [10.1109/JRPROC.1959.287136](https://doi.org/10.1109/JRPROC.1959.287136).
- [36] M. J. Frank, R. B. Nelsen, and B. Schweizer, "Best-possible bounds for the distribution of a sum – a problem of Kolmogorov," *Probability Theory and Related Fields*, vol. 74, no. 2, pp. 199–211, 1987. DOI: [10.1007/BF00569989](https://doi.org/10.1007/BF00569989).
- [37] T. L. Lai and H. Robbins, "A class of dependent random variables and their maxima," *Zeitschrift für Wahrscheinlichkeitstheorie und Verwandte Gebiete*, vol. 42, no. 2, pp. 89–111, 1978. DOI: [10.1007/BF00536046](https://doi.org/10.1007/BF00536046).
- [38] L. Rüschendorf, "Inequalities for the expectation of Δ -monotone functions," *Zeitschrift für Wahrscheinlichkeitstheorie und Verwandte Gebiete*, vol. 54, no. 3, pp. 341–349, 1980. DOI: [10.1007/BF00534351](https://doi.org/10.1007/BF00534351).
- [39] M. Abramowitz and I. A. Stegun, *Handbook of Mathematical Functions: With Formulas, Graphs, and Mathematical Tables*, 10th Ed. 1972.
- [40] P. Embrechts, A. Höing, and A. Juri, "Using copulae to bound the value-at-risk for functions of dependent risks," *Finance and Stochastics*, vol. 7, no. 2, pp. 145–167, Apr. 2003. DOI: [10.1007/s007800200085](https://doi.org/10.1007/s007800200085).
- [41] K. Binmore and J. Davies, *Calculus: Concepts and Methods*. Cambridge University Press, 2001. DOI: [10.1017/cbo9780511802997](https://doi.org/10.1017/cbo9780511802997).
- [42] A. Beck, *Introduction to Nonlinear Optimization, Theory, Algorithms, and Applications with MATLAB*. Society for Industrial and Applied Mathematics (SIAM), Oct. 2014. DOI: [10.1137/1.9781611973655](https://doi.org/10.1137/1.9781611973655).
- [43] W. Lee and J. Y. Ahn, "On the multidimensional extension of countermonotonicity and its applications," *Insurance: Mathematics and Economics*, vol. 56, pp. 68–79, May 2014. DOI: [10.1016/j.insmatheco.2014.03.002](https://doi.org/10.1016/j.insmatheco.2014.03.002).